

Microstructural, Raman, EPMA and X-ray Tomographic Study of the Odisha's Beryl (Emerald) Sample

Jena PR and Mishra PK*

CSIR-Institute of Minerals and Materials Technology, Odisha, India

Abstract

This study presents Optical, Microstructural, EPMA and X-ray tomography studies of the chromium-containing Beryl samples of Bangiriposi, Mayurbhanj district of Odisha. The detailed microscopic studies followed by EDAX analysis of different phases revealed the presence of beryllium aluminium silicate as the major matrix with yttrium silicate, Apatite, Albite, Quartz, Zircon, Cordierite and Ferichromite as minor inclusions. Micro-Raman data of the polished surface established the presence of gaseous (CO₂, CH₄), Water, and other Minerals. Few rare earth (lanthanides) elements such as Ce, Nd, Gd, Y and Sc, along with other transitional elements such as Ti and Zr, Cs are found to be present in these beryl samples. The volume percentage of silicate, phosphate, and oxide, as well as gaseous inclusions, are determined by X-ray tomographic study and are found to be 24%, 3.122% and 6.717% respectively.

Keywords: Emerald, Microstructural; Optical; X-ray tomographic studies; EPMA; Lanthanides

Introduction

Properties of beryl emerald

Beryl (Be₃Al₂Si₆O₁₈) is a beryllium ring silicate that is composed of six-membered rings of [SiO₄]₄-tetrahedral and it crystallizes in the hexagonal crystal system with P6/mcc symmetry [1]. Of these, beryl variety a chromium-bearing variety of beryl, otherwise called as Emerald (Be₃Al₂Si₆O₁₈:Cr) contains vanadium, beryllium, iron, chromium. The refractive index, density and hardness of Emerald of different origin varies in between 1.56-1.60, 2.67-2.78 and 7.5-8.0 respectively. It is available in various colors such as yellowish-green, bluish-green, blue and red. Emerald, the green gem variety of beryl, is the third most valuable gemstone (after diamond and ruby) found in the world. Colombia and Brazil supply 60% and 10% of the world's emeralds respectively.

Emerald deposits

Ancient civilizations in Africa, Asia, and South America independently discovered emerald. Emeralds were also mined in Afghanistan, Australia, Austria, Bulgaria, China, India, Madagascar, Namibia, Nigeria, Pakistan, South Africa, Spain, Tanzania, the United States, and Zimbabwe. Geology of the main emerald deposits are available in the gemmological and geological literature [2]. Similarly, India has emerald deposits in Rajasthan (Bhubani and Rajghar mines in Ajmir) and Kalaguman and Tekhi mines in Udaipur district. In Odisha, it found over a tract extending from Birmahajapur to Patnagaradh in Kalahandi district. Recently the Emerald deposits have been reported in Bangiriposi of Mayurbhanj District of Odisha. Emerald deposits have also reported from any other states including State of Andhra Pradesh, Bihar, Tamilnadu, and Jammu kashmir etc.

Emeralds with different schist

It is observed in various host rocks/schist such as tremolite, sandstone. Granitic pegmatite, sandstone, and C stone, etc. About 1.1 cm long Emeralds, in calcite and shale matrix, which found from Coscuez Mine, Muzo, Colombia. From Malyshevskoye Mine, Sverdlovsk Region, Southern Ural, similarly ~ 21 mm in length emerald crystals are present in Russia, in mica schist whereas Emerald crystal. From the Kagem Emerald (6.5 cm length) Mine, Zambia exists on a

matrix of quartz and mica schist. These crystals are blue-green colour and medium dark tone that is common in many emeralds mined in Zambia.

Colour of emerald samples

Emerald samples from Colombia, China, Zambia, and Afghanistan are found either yellowish-green, bluish-green, blue in colour. Emeralds from India are primarily green and greenish blue in nature. Recently a Red Emerald gemstone has been reported which is contrarily called as Red Beryl or Bixbite. This variety is the rarest of all beryl gemstones and exists in 12000:1 for Green to red variety. This rareness is a result of the unique conditions under which it was formed. To date, there is only one known location of gem-quality Red Emerald gemstones in the world: The Ruby Violet Mine, in the Wah Wah Mountains of South West Utah, USA [3].

Emeralds Gemstones from other places are known to be characterized by many techniques such as Micro-Raman, UV-Visible spectrophotometer, Ion chromatography, X-ray Photoelectron Spectroscopy (XPS), Particle Induced X-ray Emission (PIXE), Fourier Transform Infrared Spectroscopy (FTIR), X-ray Powder Diffraction (XRD), X-ray Tomography, Energy Dispersive X-ray Fluorescence (EDXRF), Electron Probe Micro Analyzer (EPMA), Laser-induced breakdown spectroscopy (LIBS) etc. are known to be used [4-12]. CSIR-IMMT Bhubaneswar has studied the Rough gemstone processing as well as characterisation has been carried out last three years [12-23]. Recently characterization data by DRS, Photoluminescence, XRD and chemical analysis by ICP-OES techniques have been reported from this laboratory [12]. In this article further emphasis has been given for inclusion study of the new emerald deposits found in Bangiriposi, Odisha using Microscopic techniques, EPMA, Raman as well as X-ray tomography. Details data are discussed here.

*Corresponding author: Mishra PK, CSIR-Institute of Minerals and Materials Technology, Odisha, India, Tel: 0674 237 9401; E-mail: pmimmt10@gmail.com

Received April 11, 2017; Accepted April 20, 2017; Published April 26, 2017

Citation: Jena PR, Mishra PK (2017) Microstructural, Raman, EPMA and X-ray Tomographic Study of the Odisha's Beryl (Emerald) Sample. J Geol Geophys 6: 288. doi: [10.4172/2381-8719.1000288](https://doi.org/10.4172/2381-8719.1000288)

Copyright: © 2017 Jena PR, et al. This is an open-access article distributed under the terms of the Creative Commons Attribution License, which permits unrestricted use, distribution, and reproduction in any medium, provided the original author and source are credited.

Materials and Methods

Emerald pieces of Bangiriposi area having the distinct colour difference, i.e., green (Gem#1) and greenish black (Gem#2) (Figures 1 and 2) are used for the optical, Microstructural (EPMA with EDS), Micro-Raman and X-ray Tomographic studies, etc.

UV-visible spectroscopic studies

UV-Visible spectra were obtained on UV-Visible spectrophotometer (Cary 100) with a range from 250 nm to 600 nm in DRS mode.

Micro-Raman studies

Non-polarized micro-Raman spectra have been obtained in nearly backscattering geometry between 200 cm^{-1} to 1600 cm^{-1} using a high sensitivity low noise CCD detector by In Via Renishaw make Raman spectrometer (Model no RL532C) is equipped with 5X, 20X, 50X and 100X objectives and a motorized x-y stage. Diode laser of 532 nm (visible) line and the 785 nm (IR) line have been used as excitation the source and is equipped with a sensitive detector (CCD). The laser spot diameter is $2\text{ }\mu\text{m}$. Spectra were collected using the extended scanning mode ranging from $400\text{--}4000\text{ cm}^{-1}$ and 10 s accumulation time using

lance model is Leica DM 2700M, and the data were analyzed using Wire 4.0 software.

Optical microscopic studies

Optical microscopic studies of the sample (thin section) were carried by using model 90i Nikon microscope in bright field mode and image analysis was carried out using NIS-D software. The images were obtained in both reflections as well as in transmission mode. Besides, standard photographs of the samples in taken by gemmologist microscope using halogen light.

Electron probe microanalysis studies

EPMA studies of the typical emerald samples in polished form have been carried out using EPMA (In Via JEOL, Model no. JXA8200). Images were obtained in both SEI and BSE mode. All the samples were carbon coated before analysis is done.

X-ray tomography studies

3D characterization of Green coloured Emerald sample was performed with sub-micron level Resolution X-ray CT scanner (Sky Scan 2211) in combination with the flexible 3D analysis using Avizo 9.0 software which provides the necessary photo physical parameters of the scanned samples in 3D. The object to source distance is kept at 24.724 cm and the sample is exposed for 270 ms at 68 kV and 58 μA . In this method, porosity, pore size distribution, grain size, grain orientation and surface analysis, the results of a 3D analysis can also be visualized. But here the volume percentage distributions of different phases have been calculated.

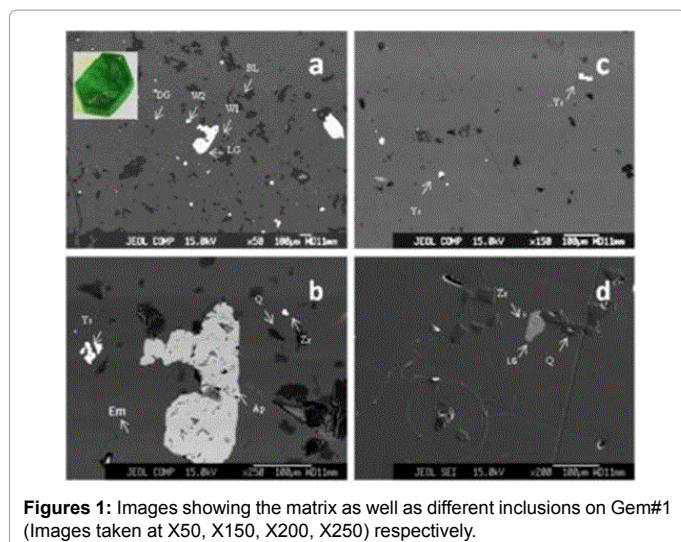
Results

Visually two types of emerald samples were taken for Microstructural analysis, a) green colour (Gem#1) and b) greenish black colour (Gem#2). FESEM images in BSE mode were taken in polished Gem#1 and Gem#2 sample (Figures 1 and 2). Figures 1a-1d shows the presence of different inclusions in Gem#1 sample whereas the Figures 2a-2d shows that for the Gem#2 samples. Tables 1 and 2 give the EPMA data of different inclusions marked in Figures 1a-1d and Figures 2a-2d respectively. X-ray image analysis has also been carried out (not shown here). Figures 3a-3d show X-ray tomographic image of the surface as well as the internal inclusion including the schist. The surface is displayed in Figure 3a whereas inclusions of different densities are shown in Figures 3b and 3c. The inclusions along with the schist are seen in Figure 3d and Figures 4a and 4b shows the optical micrograph of the oxide and phosphate inclusions both in reflection as well as transmission mode respectively. Figures 5a and 5b show flaky mica inclusion and bamboo-like structure (actinolite) respectively. Figure 6 shows the presence of crystalline inclusions at different places in transmission mode. Various crystallite present in different shape and size and crystal structure such as irregular needle-like, blade-like, layered structures containing dark opaque crystals, transparent crystals, rectangular, triangular shaped solid crystals, bamboo-like structures in detail (present in Figure 6) is shown in Figure 7 in magnified form.

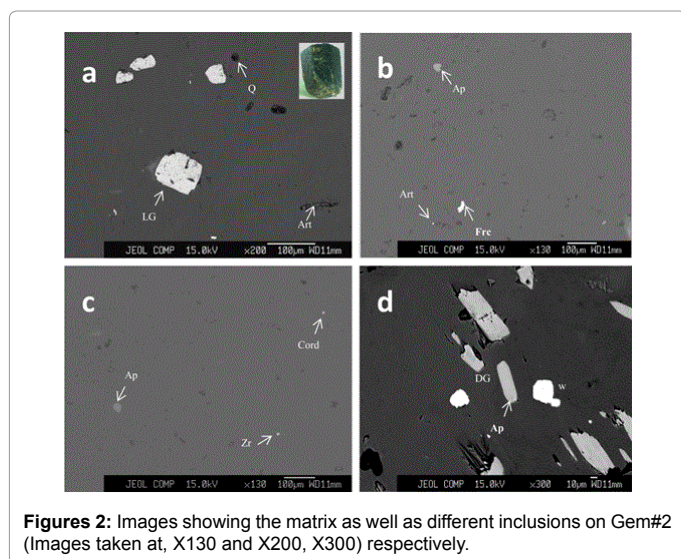
Discussion

FESEM studies with EPMA data analysis of the inclusions

Two types of emerald samples were taken for Microstructural analysis, a) green color (Gem#1) and b) greenish black color (Gem#2). UV-Visible spectral data reveals that both the samples absorb at centered around 320 nm, 430 nm and 630 nm. The later bands are due to the presence of Cr^{3+} ions whereas the bands ranging from 315-330



Figures 1: Images showing the matrix as well as different inclusions on Gem#1 (Images taken at X50, X150, X200, X250) respectively.



Figures 2: Images showing the matrix as well as different inclusions on Gem#2 (Images taken at, X130 and X200, X300) respectively.

	Gem #1	Na ₂ O	K ₂ O	CaO	MgO	Al ₂ O ₃	SiO ₂	FeO	MnO ₂	ZnO	TiO ₂	Nd ₂ O ₃	ZrO ₂	F	Cl	Sc ₂ O ₃	P ₂ O ₅	Y ₂ O ₃	Gd ₂ O ₃	Ce ₂ O	Cr ₂ O ₃	
Figure 1(b)	Dark Gray (DG)	2.3	-	-	5.05	22.67	70.85	-	-	-	-	-	-	-	-	-	-	-	-	-	-	-
	W1	-	-	-	-	-	34.9	-	-	-	-	-	65.1	-	-	-	-	-	-	-	-	-
	W2	-	-	8.65	-	8.38	42.54	7.78	-	-	-	-	-	-	-	-	-	32.65	-	-	-	-
	Light gray (LG)	-	-	50.19	-	-	-	-	-	-	-	-	-	-	-	-	49.81	-	-	-	-	-
	Black (BL)	-	-	-	-	-	100	-	-	-	-	-	-	-	-	-	-	-	-	-	-	-
Figure 1(c)	W1	-	-	9.02	-	-	46.2	8.41	-	-	-	-	-	-	-	-	-	27.92	8.45	-	-	-
	W2	-	-	4.53	5.6	-	42.08	8.88	-	-	-	-	-	-	-	-	9.12	29.79	-	-	-	-
Figure 1(d)	W1	-	-	-	-	-	35.54	-	-	-	-	-	64.46	-	-	-	-	-	-	-	-	-
	Light gray	-	-	15.21	1.32	18.64	32.08	10.02	-	-	0.39	6.17	-	-	-	-	-	-	-	-	15.53	-
	Dark Gray	-	-	4.94	18.88	73.99	2.19	-	-	-	-	-	-	-	-	-	-	-	-	-	-	-
	Black	-	-	-	-	-	100	-	-	-	-	-	-	-	-	-	-	-	-	-	-	-

Table 1: Gem #1 EPMA analysis.

	Gem #2	Na ₂ O	K ₂ O	CaO	MgO	Al ₂ O ₃	SiO ₂	FeO	MnO ₂	ZnO	TiO ₂	Nd ₂ O ₃	ZrO ₂	F	Cl	Sc ₂ O ₃	P ₂ O ₅	Y ₂ O ₃	Gd ₂ O ₃	Ce ₂ O	Cr ₂ O ₃	
Figure 2(a)	Light gray (LG)	3.04	6.18	0.77	2.3	11.64	24.11	22.19	1.3	-	-	-	-	-	-	0.46	-	-	-	-	-	33.98
	Dark Gray (DG)	9.37	-	1.61	4.78	9.89	76.58	2.98	-	-	-	-	-	-	-	0.21	-	-	-	-	-	-
	Black	-	-	-	-	-	100	-	-	-	-	-	-	-	-	-	-	-	-	-	-	-
Figure 2(b)	W1	-	-	-	-	-	-	65.99	-	-	-	-	-	-	-	-	-	-	-	-	-	34.01
	W2	3.18	-	-	4.97	22.24	66.23	3.28	-	-	-	-	-	-	-	-	-	-	-	-	-	-
Figure 2(c)	Light gray (LG)	-	-	84.08	-	-	-	-	-	-	-	-	-	5.38	-	-	10.54	-	-	-	-	-
	W1	-	-	-	5.42	17.44	77.14	-	-	-	-	-	-	-	-	-	-	-	-	-	-	-
	W2	-	-	-	-	5.27	46.68	-	-	-	-	-	48.05	-	-	-	-	-	-	-	-	-
Figure 2(d)	Light gray (LG)	-	-	62.04	-	-	-	-	-	-	-	-	-	-	-	-	37.96	-	-	-	-	-
	W	-	-	-	-	0.87	-	60.82	1.41	2.44	0.18	-	-	-	-	-	-	-	-	-	-	32.91
	Dark Gray (DG)	1.14	-	-	4.55	16.15	75.36	2.5	-	-	-	-	-	-	-	-	-	-	-	-	-	1.5

Table 2: Gem#2 EPMA analysis.

nm centered around 320 nm may be due to charge transfer of O²⁻ to Fe³⁺ in the tetrahedral site of the Be²⁺ site. Figures 1a-1d shows the presence of different inclusions in Gem#1 sample whereas the Figures 2a-2d shows for the Gem#2 samples. It has been observed that different types of silicate, oxide and phosphate inclusions are present in Gem#1 samples. Figure 1a shows the matrix as well as different inclusions (Images were taken at X50) and they are Dark gray, Light gray, white and black and are marked as DG, LG, W1 and W2 and BL (Figures 1a-1d). Figure 1b shows a magnified version (images taken at X250) of the inclusion shown in Figure 1a. EPMA analysis has been carried out for each of these inclusions, and they are represented in oxide form and shown in Table 1. From the EPMA data, these inclusion are found to be rich in aluminium silicate, apatite, zirconium silicate (zircon), cordierite, phases rich in yttrium silicate with the minor amount of CaO, MgO and FeO (in oxides form) and quartz. The presence of beryllium in the DG matrix has been observed from the ICPES data

(not reported here). Hence the matrix is of Emerald and marked phases are different inclusions with shape and size distributed in the emerald matrix. It has also been found that composition of all the white colored phases (W1 and W2) with very small size (<1 micron) are distributed throughout the matrix) are not same viz. W1 phase shown in Figures 1b and 1d are found to be pure form of Zircon containing 34.9 (SiO₂), 65.1 (ZrO₂) and 35.54 (SiO₂), 64.46 (ZrO₂) respectively whereas both W1 and W2 phases are rich in yttrium silicate (shown as Ys in Figure 1c) with a minor percentage of CaO, MgO, P₂O₅, Gd₂O₃ and FeO (Table 1). DG and LG inclusions are found to be rich in alkaline feldspar and apatite inclusions respectively. Rare earth elements such as Nd₂O₃, Ce₂O₃ besides CaO, MgO, FeO with TiO₂ are found in typical light gray colored inclusions (Figure 1c), whereas the BL marked, inclusions are a pure form of Quartz (Figures 1b and 1d). It is to be noted that the Gem#2 does not contain rare earth element instead it contains Sc₂O₃ (vide infra).

Similarly, for Gem#2 sample detailed EPMA analysis has been carried out for each of Dark Gray (DG), Light Gray (LG), white (W) and black (BL) (marked in Figures 2a-2d) and data are given in Table 2. Here also different types of silicate, oxide, phosphate phases are present Quartz is found in pure form (shown as BL) whereas unlike in Gem#1 sample it contains Zircon with minor percentage of alumina in it. EPMA data reveals that Ferichromite, Zircon (Zr), Apatite (Ap), Quartz (Q), cordierite (Cord), Aerinite (Art) and alkali feldspar are present in this sample and they are given in Table 2 and marked in Figures 2a-2d. From EPMA data all the white coloured inclusions are not same instead the W1 phases shown in Figures 2b and 2d are Ferichromites with the minor quantity of MnO, ZnO, and TiO₂ whereas, W1 shown in Figure 2c is calcium aluminium silicate. Both the light

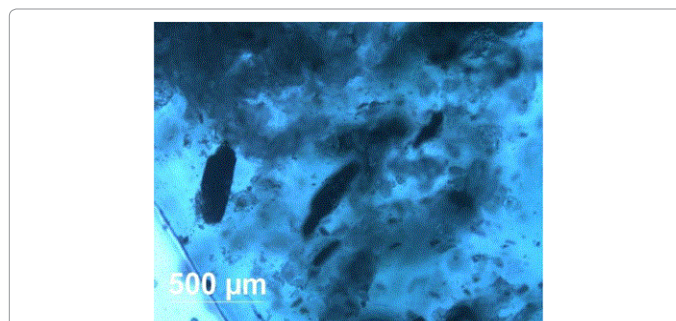


Figure 6: Optical micrograph of the inclusions in Emerald in transmission mode.

gray coloured inclusions shown in Figures 2b and 2c are apatite with or without minor percentage of fluoride in it. Besides alkali feldspars with or without Cr₂O₃ and Sc₂O₃ are found in light gray and dark gray colored inclusions. Detailed EPMA data are given in Table 2. Although Cs has not been found ICPES data (not shown here) showed the presence of Cs in it. Unlike in green coloured (Gem#1). In this case Zircon is found with minor percentage of alumina in it. As discussed earlier the matrix also contains Emerald phase. Unlike observed in Figures 2a-2c, Figure 2d shows dendritic and elongated types of phases and they are found to be apatite. Besides here also Ferichromite phase is found as the major inclusions with the minor quantity of ZnO and TiO₂. Results of X-ray mapping of these phases corroborate with the findings.

X-ray tomographic studies

X-ray micro-CT offers the advantages of non-destructive imaging of relatively large areas of high spatial resolution and can be used to feed micromechanical models. Different rotation maps revealing the distribution of different minerals across the 3D geometry reveals the presence of different minerals and voids in the gemstone matrix. It may be noted that gray scale image is computed based on the X-ray attenuation coefficient value of an element. Density or concentration of an element is the reconstructed image is dependent on the darkness of voxel in gray scale. X-ray m-CT image of Emerald sample is presented in Figures 3a-3d where a) shows the surface of the samples in gray scale and the sectional view in 2D shown in Figures 3b and 3c show the presence of the distribution of solids and pores. Figures 3d show the distribution of different minerals present in the gemstone (shown in coloured form). Besides gemstone matrix, it also shows the presence of tremolite schist attached to it. Furthermore, Figure reveals the volume of the pores present in it. However, the absence of microspores (<8 micron) could not be confirmed by the present X-ray Micro-CT since the maximum resolution offered by the instrument was 8 micron. Over every non-destructive imaging of the samples. Within this range, it has been found that there are 4 phases present (as per the density) in Emerald matrix. They are represented in grey, faint grey, white and black. The solid content in the typical matrix is 3.122 whereas, the volume of pores, cracks as well as the gaseous mixtures are up to 6.717 and rest are the matrix with two different density.

Optical microscopic and mineralogy studies

As these inclusions are basically silicate, phosphate, and oxides. Hence, few polished Emerald specimens were observed under the optical microscope in reflection as well as in transmission mode to study their mineralogy.

Figure 4 shows a typical apatite phase with silicate phases (marked as 1 and 2). The opaque silicate phases as observed under reflection mode become transparent in transmission mode whereas the apatite

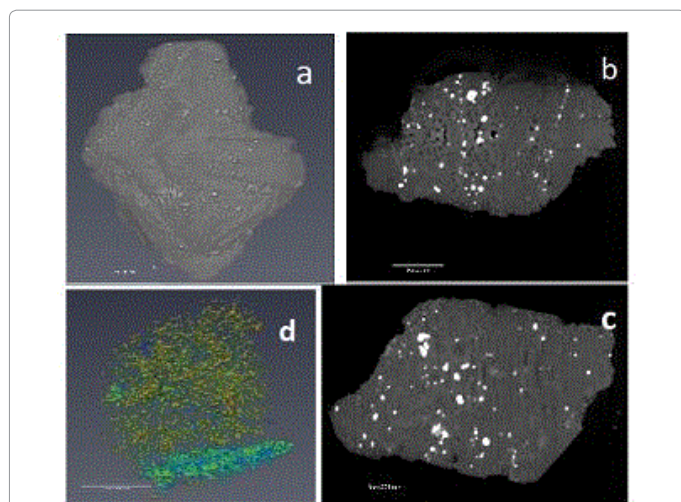


Figure 3: X-ray μ-CT image of Emerald sample is presented where it shows the surface of the samples in the sectional view in 2D shown.

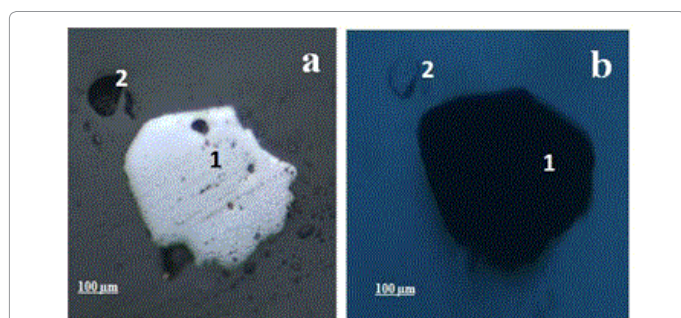


Figure 4: Optical microstructure of typical emerald sample (Gem#1) in reflection as well as transmission mode (in 100 μm).

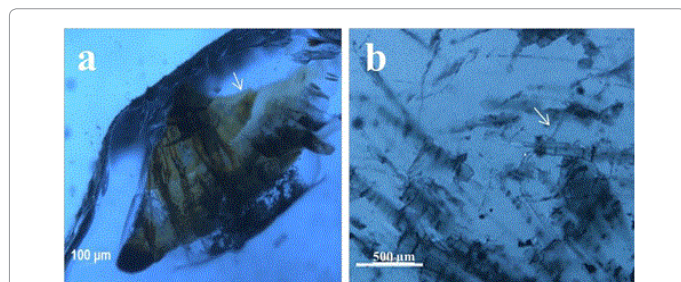


Figure 5: Optical micrograph of inclusions in Emerald showing (a) flaky like structure (b) Bamboo types actinolite (in 500 μm) respectively.

becomes opaque from the gray color. Similarly optical micrographic data of the polished form of Gem#1 and Gem#2 at different places shown similar results. A clear brown colored flaky crystals, bamboo types actinolite, are clearly seen in Figure 5. The mineralogical point of view, this could be mica and actinolite respectively. Fluid inclusions are also seen in layered like structures [vide infra]. Figure 6 shows optical micrograph of different inclusion present in Emerald where some of the inclusions are shown in magnified form (Figure 7). There are (a) rectangular transparent crystal inclusion with small gas bubble, (b) single rectangular crystals inclusion (phenakite), (c) transparent crystal with adhered dark part (albite), (d) Crystals with characteristics features of opaque elongated crystals (amphibole), (e) two-phase inclusions containing platy transparent crystal with gas in the centre, (f) a trigonal crystal (calcite), (g) transparent rectangular crystals showing layer like structure, (h) Transparent crystals containing opaque oxide coatings and (i) bunch of colourless crystals (quartz). Similar such observations were made for different emerald samples of bangiriposi area.

Raman study of the inclusions

Raman analysis data shows the presence of zircon, iron oxides and silicate phases along with type I water. Raman bands at 320 cm^{-1} , 394 cm^{-1} , 449 cm^{-1} , 527 cm^{-1} , 623 cm^{-1} , 683 cm^{-1} , 1068 cm^{-1} reported for Emerald bands. Raman peak at 320 cm^{-1} best matches the beryl Si_6O_{18} ring breathing mode. Besides additional Raman-active modes near 750 cm^{-1} (Al) and above 850 cm^{-1} (Be) are also reported, and this is due to significant mixing of Al and Be motions with those of the ring. Raman bands due to emerald as well as Zircon, are observed although Raman analysis of all these phases has been done. Figure 8 reveals the different peaks like 289 cm^{-1} (Hematite), 425 cm^{-1} (OH-Stretching), 558 cm^{-1} (Deformation of Si_4O_{11}), 668 cm^{-1} (Magnetite), 681 cm^{-1} (Si-O-Si Stretching), 971 cm^{-1} (Absorption of O-Si-O), 1009 cm^{-1} (Zircon), 3598 cm^{-1} belongs to type-I (without alkali nearby). A Raman spectrum shown in Figure 8 reveals the presence of Magnetite in emerald samples which corroborates with the mineralogical observation. Similarly, the presence of OH is also depicted from the Raman study. The presence of mica (biotite), phenakite, actinolite, quartz, tourmaline, chromite, etc. have been reported for these types of emeralds and also has been reported for emeralds of different deposits.

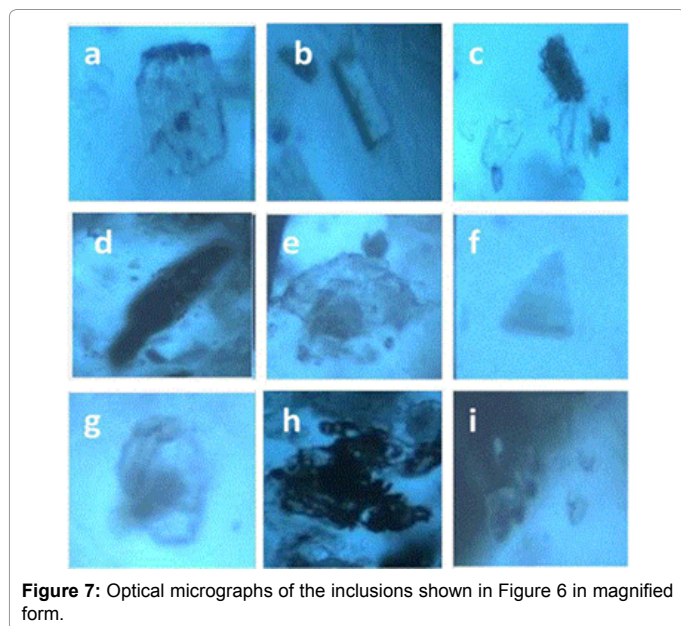


Figure 7: Optical micrographs of the inclusions shown in Figure 6 in magnified form.

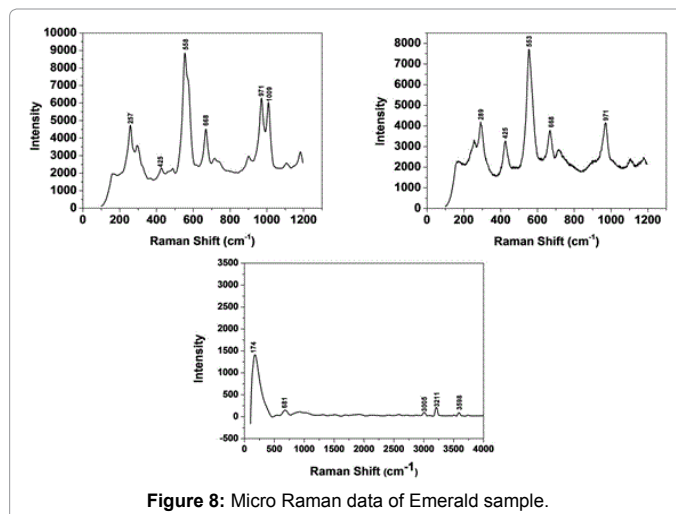


Figure 8: Micro Raman data of Emerald sample.

As reported by many authors there are three types of inclusions present in emerald, i.e., solid minerals of different category depending on the area of existence, gasses as CO_2 , CH_4 , N_2 and water as the fluid. Of these solid, fluid and gaseous inclusions in emerald have been studied for emerald of different origin by different authors. Different minerals of various shape and size having different refractive index are present as solid minerals. Of these, the presence of singly refractive solid (cubic) crystals consisting of halides, daughter Crystal identified as calcite (peaks at 283 cm^{-1} , 713 cm^{-1} and 1085 cm^{-1}), additional peaks at 2328 cm^{-1} assigned to N_2 are reported [24]. Besides, graphite, different complex mixed salt and daughter minerals are also said. In some cases, the shape of the inclusions are found to be irregular, with numerous of branches, and on rare occasions, they are of the needle-like structure. Long back Venkateswaran identified the gas phase CO_2 (peaks at 1284 cm^{-1} and 1387 cm^{-1}) in emerald by Raman spectroscopy [5].

Emeralds from Musakashi (Zambia) contain multiphase inclusions hosting not only liquid and gas bubbles but also several solid phases. Usually at least two crystals, one cubic, one more rounded, and often several smaller ones ranging from transparent colorless to opaque black are reported. In Musakashi emerald sample, the cubic crystals, the gas phase, and the daughter crystals were identified by Raman spectroscopy as a halide, CO_2 , and carbonate, respectively. Results are identical to those reported for fluid inclusions Colombian emerald. In Columbian emerald, a tiny dark opaque crystal and irregularly shaped clusters of daughter crystals are observed. These daughter crystals are related to various carbonate compounds. Most of the multiphase inclusions had the classic jagged shape. Also in several cases, the shape was more elongated, like a blade and occasionally irregular [6].

Although three-phase inclusions in samples reported from Musakashi, Zambia is similar to those in emeralds from Colombia, Afghanistan, and China (Xin Jiang) but specimens from the neighbouring Kafubu area of Zambia contain two-phase inclusions with crystals that are visible only under cross-polarized light [25]. Similarly samples from Davdar, China were found to be multiphase. These were often jagged or irregular in shape and occasionally needle-like. Some fluid inclusions contained two halide cubes [26]. In these emeralds, the gas bubble was smaller than the whole inclusion and usually somewhat smaller than the associated cubic crystals.

Indian emeralds from different places are also multiphase. Choudhary from Jaipur [27] described the inclusions of Jharkhand emerald. As mentioned above, most of these emeralds are characterized

by haziness, caused by minute inclusions, which could not be resolved under a standard gemmological microscope. However, some appeared to be colorless minerals. Further, Raman analysis identified a range of mineral inclusions (such as, actinolite (acicular blades), allanite-La (black-brown, euhedral, sub-metallic), apatite (colourless, euhedral to subhedral), beta-fergusonite (brownish-clusters), epidote (euhedral), chromite/magnetite/picotiter (black grains), mica (annite/phlogopite/chamosite/biotite-brown to colourless, elongated and platy), phenakite (colourless, clusters, subhedral), quartz (euhedral to anhedral), rutile (dark brown, subhedral), sphene (yellow, elongated crystals), zircon (rounded and with stress cracks), etc.

Similarly, emeralds from Bangiriposi area, have been reported before and there are irregular needle-like, blade-like, layered structures containing dark opaque crystals, transparent crystals, rectangular, trigonal shaped solid crystals, bamboo-like structures are found. Besides fluid inclusions are seen in the layered blade-like structures (Figure 7). Similarly, the presences of other inclusions such as water types and alkali ions have also been studied by many authors. It is known that in emerald, water is present in different types, i.e., type I and type II. These are determined by both Raman and FTIR spectroscopy. But for solid inclusions Raman spectroscopy has been reported by many authors.

Raman spectroscopy is a versatile non-destructive technique for fluid inclusion analysis, with a wide field of applications ranging from qualitative detection of solid, liquid and gaseous components to identification of polyatomic ions in solution. "Raman technique is commonly used to calculate the density of CO₂ fluids, the chemistry of aqueous fluids," and the molar proportions of gaseous mixtures present as inclusions. In Emerald type I and type II and they are related to the presence of nearby alkali ions. Study of OH stretching modes are powerful probes to investigate the presence of alkali ions in the natural beryl channels. Raman bands centered at about 3608 cm⁻¹ and 3598 cm⁻¹ belong to water type I (without alkali nearby) and water type II (with alkali nearby), respectively for natural samples. The real position of the bands may vary by only a few cm⁻¹. However, these Raman bands do not exist in this spectral region for the flux-grown synthetic crystals, which are formed in the absence of water. On the other hand, hydrothermally grown synthetic crystal display one Raman band at about 3608 cm⁻¹. The intensity ratio of 3598 and 3608 peaks depends on a number of alkali ions present in the sample. Emerald grew in contact with schist rocks usually contain more alkali ions than those coming from classical granitic pegmatite. Therefore, for 'non-schist type' emeralds, the intensity of 3608 cm⁻¹ bands should be higher than that of the band at 3598 cm⁻¹ [4].

Similarly, the presence of type I and type II water molecules can also be studied by FTIR spectroscopy. The extraordinary ray plots of type I emeralds each exhibits 7140 cm⁻¹ peak that was more intense than the peaks at 7095 cm⁻¹ and 7072 cm⁻¹. The plots from type II emeralds display their high-intensity peak at 7095 cm⁻¹ [10]. Wood and Nassau [7] and Schwarz and Henn [10] assigned the 7140 cm⁻¹ peak to type I water molecules and the 7095 cm⁻¹ peak to type II water molecules. All of the emeralds from Davdar, China contained type I water molecules except the samples from Kafubu. Indian Bangiriposi samples contain type I type water molecules.

Conclusion

The Emerald sample of Odisha has been characterized in detail by Microscopic optical techniques, EPMA as well as X-ray tomography. Various inclusions such as Albite, Ferichromite, Apatite, Phenakite, Calcite, Actinolite, Amphibole, Allanite-L, Quartz have been detected.

Besides these typical pieces reveals the presence of Y, Nd, Ce, Gd with other elements such as Zn, Ti and Zr (presented in oxide form).

Acknowledgement

Authors would like to Director for kindly giving permission to publish this paper. They also thank CSIR for funding the project on "Processing of Natural gemstones for aesthetic improvement and value addition [Esc 206]" and Mr. Papu Ranjan Jena thank CSIR for grant of fellowship under this project. The staffs of the CCC department are acknowledged for Raman and EPMA studies.

References

1. Goldman DS, Rossman GR (1977) The identification of Fe²⁺ in the M4 site of calcic amphiboles. *Am Mineralogist* 67: 340-342.
2. Groat LA, Giuliani G, Marshall DD, Turner D (2008) Emerald deposits and occurrences: A review. *Ore Geol Reviews* 34: 87-112.
3. Shigley JE, Thompson TJ, Keith JD (2003) Red Beryl from Utah: A review and update. *Gems and Gemol.*
4. Bersani D, Azzi G, Lambruschi E, Barone G, Mazzoleni P, et al. (2014) Characterization of emeralds by micro-Raman spectroscopy. *J Raman Spectrosc* 45: 1293-1300.
5. Venkateswaran CS (1935) The Raman spectra of some metallic halides. *Proceedings of the Indian Academy of Sciences* 1: 850-858.
6. Giuliani G, Cheilletz A, Dubessy J, Rodriguez CT (1993) Chemical composition of fluid inclusions in Colombian emerald deposits. 8th Quadrennial IAGOD Symposium pp: 159-168.
7. Wood DL, Nassau K (1968) The characterization of beryl and emerald by visible and infrared absorption spectroscopy. *Am Mineralogist* 53: 777-799.
8. Yu KN, Tang SM, Tay TS (2000) PIXE studies of emeralds. Department of Physics, National University of Singapore 29: 267-278.
9. Tang SM, Tang SH, Mok KF, Retty AT, Tay TS (1989) A study of natural and synthetic rubies by PIXE. Department of Physics, National University of Singapore 43: 219-222.
10. Schwarz D, Henn U (1992) Emeralds from Madagascar. *J Gemmol* 23: 140-149.
11. Gilberto A, Romano R, Kenny S, Pier FZ (1993) Structure refinements of beryl by single-crystal neutron and X-ray diffraction. *Am Mineral* 78: 762-768.
12. Reshma B, Sakthivel R, Mohanty JK (2016) Characterization of low-grade natural emerald gemstone. *J Geol Geophys* 6: 271.
13. Sinha J, Mishra P (2015) Spectroscopic and microstructural studies of ruby gemstones of Sinapalli, Odisha. *J Geol Soc India* 86: 657-662.
14. Swain S, Pradhan SK, Jeevitha M, Acharya P, Debata M, et al. (2016) Microwave heat treatment of natural ruby and its characterization. *Applied Phys A* 122:1-7.
15. Sahoo RK, Mohapatra BK, Singh SK, Mishra BK (2014) Influence of temperature on surface coloration of the lead oxide treated natural gem ruby. *Ad Sci Letter* 20: 622-625.
16. Sahoo RK, Mohapatra BK, Singh SK, Mishra BK (2015) Aesthetic value improvement of the ruby stone using heat treatment its synergetic surface study. *Applied Surface Sci* 329: 23-31.
17. Das SK, Mohanty JK (2014) Characterisation of Eluvial corundum (Ruby) from Kermunda, Kalahandi District, Odisha, India. *Geol Geosci* 3: 3-6.
18. Pradhan C, Sakthivel R, Dash T, Nayak BB, Mishra BK (2015) Effect of waller solution and lemon juice treatment on photoluminescence behaviour of low-grade ruby. *K Int J Chem Res* 516: 1-17.
19. Nayak BB, Dash T, Mishra BK (2016) Purple coloured natural ruby: X ray photoelectron spectroscopy, X-ray diffraction, X-ray tomography and other microstructural characterizations. *Int J Sci: Basic and Applied Res* 25: 94-114.
20. Sahoo RK, Mohapatra BK, Singh SK, Mishra BK (2016) Aesthetic value addition and surface study of Odisha ruby stones by heat treatment with different metal oxide additives. *Adv Sci Letter* 22: 340-344.
21. Sahoo RK, Singh SK, Mishra BK (2016) Surface and bulk 3D analysis of natural and processed Ruby using electron probe microanalyzer and X-ray micro-CT scan. *J Electr Spectrosc Related Phenomena* 211: 55-63.
22. Sahoo RK, Singh SK, Mishra BK (2016) Aesthetic enhancement of the low-quality waste gemstones to a high-value product by modified thermal diffusion. *Waste* 53: 1-5.

-
23. Rout PP, Sahoo RK, Singh SK, Mishra BK (2017) Spectroscopic investigation and color change of natural topaz exposed to PbO and CrO₃ vapour. *J Vibrational Spectrosc* 88: 1-8.
24. Saeseaw S, Pardieu V, Sangsawong S (2014) Three-phase inclusions in Emerald and their impact on origin determination. *Gems Gemol*.
25. Zwaan JC, Seifert AV, Vrána S, Laurs BM, Anckar B, et al. (2005) Emeralds from the Kafubu area, Zambia. *Gems Gemol* 41: 116-148.
26. Marshall D, Pardieu V, Loughrey L, Jones P, Xue G (2012) Conditions for emerald formation at Davdar, China: Fluid inclusion, trace element, and stable isotope studies. *Mineralogical Mag* 76: 213-226.
27. Choudhary G (2015) Emeralds from Jharkhand, India: An update Gem Testing Laboratory, Jaipur, India.